Macromolecular Research Article

DOI 10.1007/s13233-019-7039-y www.springer.com/13233 pISSN 1598-5032 eISSN 2092-7673

An Insight Into the Physico-Mechanical Signatures of Silylated Graphene Oxide in Poly(ethylene methyl acrylate) Copolymeric Thermoplastic Matrix

Sayan Ganguly[1]
Subhadip Mondal[1]
Poushali Das[2]
Poushali Bhawal[1]
Tushar Kanti Das[1]
Sabyasachi Ghosh[1]
Sanjay Remanan[1]
Narayan Chandra Das*[,1,2]

[1] Rubber Technology Centre, Indian Institute of Technology, Kharagpur 721302, India
[2] School of Nanoscience and Technology, Indian Institute of Technology, Kharagpur 721302, India

Received May 9, 2018 / Revised August 9, 2018 / Accepted August 30, 2018

Abstract: Dispersion of graphene as nano-building block in polymer matrix is challenging for developing high strength polymer nanocomposites. Tuning of surface polarity can be an effective pathway to resolve this issue of dispersion. Besides this, the polymer matrix (Ethylene methyl acrylate or EMA) has been chosen here judicially due to its polar-nonpolar alternating copolymeric segments which indirectly facilitated dispersion of nanofillers. Herein, graphene oxide has been lyophilically modified by virtue of surface grafting phenomenon with the help of di-halo substituted silane. The most surprising outcome which has been nurtured is their superior dispersion, improvement in physico-mechanical features, and transparency without affecting the inherent compliance of pristine polymer. The transmission electron microscopic image of silane functionalized graphene oxide (GOF) is showing surface roughness which has immense effect of physisorption and mechanical anchoring of polymer chains over GOF nano-sheets. Such physical interaction has enough impact on mechanical properties which has been discussed here. Moreover, the deterioration of transparency was not so much affected after loading of GOF filler. The filler distribution also has been confirmed in the light of small angle X-ray scattering (SAXS) study. Thermal treatment has been conducted for composites which accounted high thermal stability comparatively to pristine polymer.

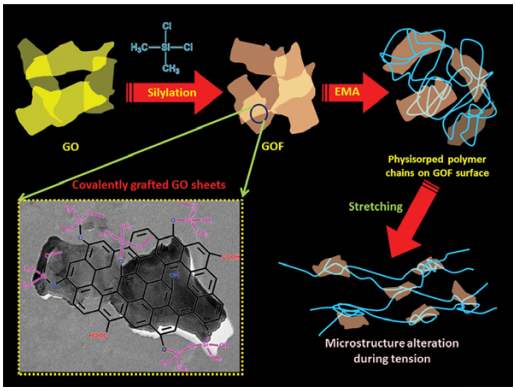

Keywords: lyophilically modified, mechanical anchoring, transparency, SAXS.

1. Introduction

Graphene is an immensely uttered material in the multidisciplinary sciences due its outstanding stiffness, superior strength, electrical and thermal conductivity and several unique physical features.[1-4] The insertion of graphene into polymer matrix bears exceptional mechanical properties and milt-functional characteristics which can be a suitable alteration of traditional carbon nanotubes. Various researchers already proposed the superiority of graphene in polymer matrix on account of their stiffness, fracture toughness, fatigue, electrical and thermal properties after modification of graphene.[5-12] But the major demerit of the graphene as a filler is its high aspect ratio, surface area and strong van der Waals force of attraction. These inherent features of graphene are very much prone to form agglomeration and large fractal type morphology. These also are the problems for uniform dispersions, lack of mechanical properties and desirable interfacial interactions between the filler and polymer matrix.[13-15] To ensure improved dispersion and long range homogeneity in the polymeric matrix, a good interfacial interaction among the graphene platelets and polymer chains have utmost necessity. As a macroscopic result, these interfacial interactions have the key role for a composite to be mechanically robust against applied forces.[16-18]

After surveying the graphene based composites, in general two forms of graphene are mainly used; one is graphene oxide (GO) and another is reduced formed of GO. The polarity of the graphene based form has been nurtured before filling into a polymer. The GO has a variety of polar functionalities of its basal planes and through the edges.[19] The polar functionalities present in the GO become a platform for surface modifications. Surface modification of GO is normally a process to tune up the polarity of the graphene sheets. Since the last few decades, there are several works were practiced on GO surface treatment and functionalization to improve dispersion, interfacial interaction and mechanical properties.[20-24] Among these covalent functionalizations, silane coupling agents were used to modify the GO surface for the enhancement of their compatibility to the

Acknowledgments: N. C. Das would like to thank to the Science and Engineering Research Board (SERB), Department of Science and Technology (DST), Ministry of Science and Technology, Govt. of India (ECR/2016/000048) for financially supporting this work sincerely.

***Corresponding Author:** Narayan Chandra Das (ncdas@rtc.iitkgp.ac.in)

polymer matrix as well dispersion.[25-27] In this coupling process, hydroxyl groups react with silane without affecting the remaining functional groups. Silanes are basically grafted on to surface of graphene sheets by covalent linking which have an impact on the dispersibility of the graphene in polymer matrix. Yang *et al.* used an amine functionalized silane for covalent grafting of GO which can increase the compressive strength of graphene-polymer composite with effective dispersion and compatibility.[28] In another work, Lin and his coworkers showed silane grafted GO as a compatible filler for maleic anhydride modified polypropylene with a very low filler loading.[29] Such silane modified GO was also been studied by Wang *et al.* in epoxy matrix with which leads to the high tensile property. The dispersion and interfacial interaction was also enhanced by others silanes by solution grafting process.[30,31] Sometimes silanes were also grafted to carbon nanotubes to enhance better mechanical properties of the polymer matrix which is reported elsewhere.[32]

Ethylene methyl acrylate (EMA) had been chosen here as a polymer matrix. The cause of this choice is its commercial availability, ageing resistance, good weather resistance, high strength to weight ratio compared to other commercially available plastics, low temperature flexibility without application of plasticizers and desirable translucency.[33-35] EMA consists of acrylate segments as well ethylene domains which are slightly polar as well nonpolar portions respectively. Such alteration is helpful for dispersion of filler into matrix. That's why EMA had been chosen here to carry forward the experimentations to prove the applicability of functionalized GO nanofillers.

After a thorough literature survey about this silane modified GO impregnated polymer composites, we noticed maximum works has been done on the thermoset polymer matrix systems. Thermoplastic matrixes were not nurtured in-depth for the silane modified GO filled thermoplastic systems. From this viewpoint we were inspired to develop such modified graphene filler based thermoplastic matrix with good dispersion and good mechanical properties. The agglomeration effect of GO in thermoplastic matrix is a common problem during solution mixing method. These types of drawbacks can be avoided by using such organiphilic fillers. The mechanical strength also gives another impact in the enhancement of compatibility/miscibility as well as strength bearing capability of the as developed nano-composites where graphene sheets play a role in stress transfer point. Herein, we used dichlorodimethylsilane (DCDMS) as a covalently surface modifying agent. This DCDMS can graft on the graphene sheets through convalent condensation reaction among the hydrophilic functional groups. The thermal and mechanical properties of the composites were evaluated to establish the silane modification effect.

2. Experimental

2.1. Materials

Commercial grade of ethylene methyl acrylate (EMA) (Elvaloy® 1330; DuPont) was procured with 30 wt% methyl acrylate content, melt flow index 3 g/10 min. and density of 0.95 gm/cm^3. Dichlorodimethylsilane (DCDMS) was purchased from Sigma. Graphite and other chemicals were purchased in analytical grade from loba chemie.

2.2. Synthesis and functionalization of graphene oxide

GO was prepared from the naturally occurring graphite flakes following our previous work.[36] The GO was ultrasonicated for 4 h to obtain a highly exfoliated GO water dispersion. Silane functionalization of GO was done after following the procedure depicted in Figure 1. Concisely, 120 mL toluene and 200 mg GO (solid) were taken in a three-neck round bottom (RB) flask and sonicated for 45 min. After that, DCDMS was added as per the formulation given in Table 1. Then the DCDMS mixed GO disper-

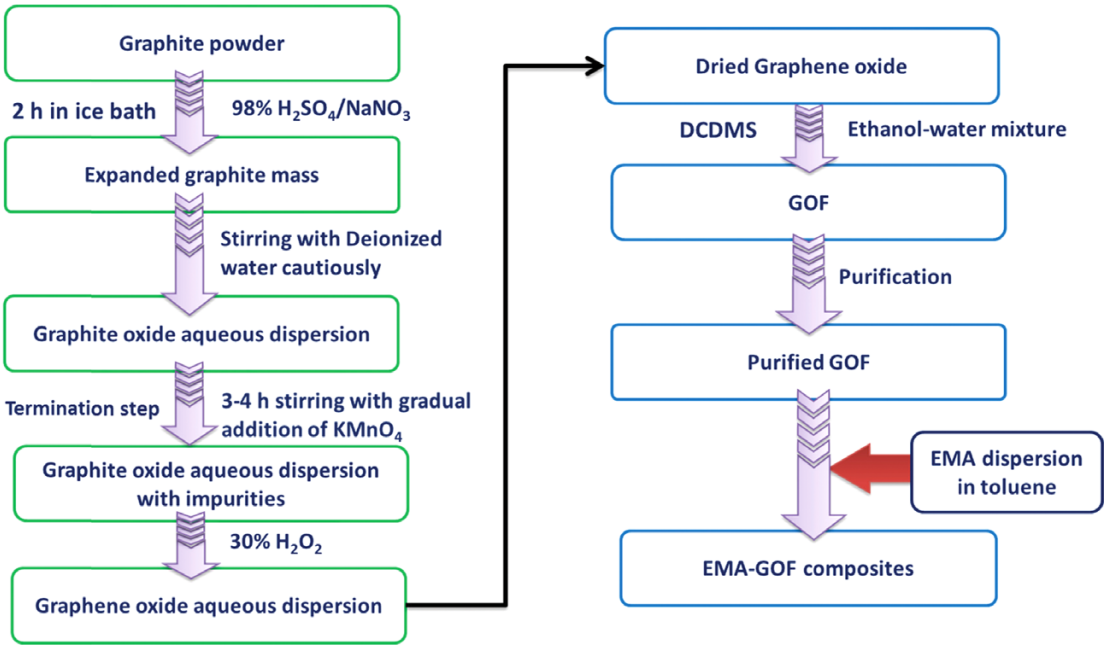

Figure 1. Diagrammatic representaion of preparation of GOF and fabrication of EMA-GOF nanocomposites.

Table 1. Formulation nomenclature of the prepared EMA-GOF nanocomposites

Code	GO (g)	DCDMS (mL)	GOF (g)	EMA (g)	Filler loading (wt%)
F0	-	-	-	5	0
F1	0.6	5	0.05		1
F2			0.15		3
F3			0.25		5
F4		10	0.05		1
F5			0.15		3
F6			0.25		5
F7		15	0.05		1
F8			0.15		3
F9			0.25		5

sion was stirred for 3 h at room temperature followed by 3 h at 100 °C with nitrogen atmosphere. The solid dispersion was then centrifuged and washed thoroughly by toluene and water-ethanol (10/90 V/V) mixture to remove the excess amount of reacted silane. After that the solid powder was dried under vacuum over at 70° for overnight. The as prepared product was named silane functionalized GO or shortly GOF.

2.3. Fabrication of GOF-EMA nanocomposites

GOF filled EMA based nanocomposites were prepared by solution mixing technique. The desired amount GOF was primarily dispersed in toluene (80 mL) by sonication for 45 min in room temperature. After that a black coloured mixture was obtained and it was denoted as set I. In a separator beaker specific amount of EMA was dissolved in 80 mL toluene at 60 °C and denoted as set II. After fully dissolution of EMA, the set I was poured into the set II very slowly with vigorous stirring. The mixing procedure was continued for 30 min. The slow mixing was adopted to avoid agglomeration of the set I into the set II and proper exfoliation of set I in the EMA matrix.[37] After complete addition of the set I into set II, the total system was subjected to stirring at same temperature (60 °C) for another 1 h. After that the mixed system was casted in a Teflon coated petrie-dish and rested for overnight for air dry. Then the casted petrie-dish was vacuum dried at 80 °C for 12 h. For comparison, neat EMA was also processed likewise. The dried composites and neat EMA were then cut into small pieces and molded at 5 MPa, 140 °C for 5 min. in a compression molding machine (Moore press, UK) attached water cooling unit. The average thickness of the sheets was ~1 mm.

2.4. Characterization

Fourier transformed infrared spectra of GO, GOF and EMA-GOF composites were performed in ATR mode on a Perkin-Elmer FTIR spectrophotometer (4000-500 cm^{-1}, 16 scans). Raman spectra were evaluated by using Trivista 555 spectrograph (Princeton Instruments, 647 nm Kr^+ laser; Coherent, Sabre Innova SBRC-DBWK) with the power around 10-12 mW for 120 s in the spectrum range of 1000-2000 cm^{-1}. Wide angle X-ray was done on an X-ray diffractometer (X'Pert PRO, made by PANalytical B.V., The Netherlands) using Ni-filtered Cu-K_α (λ=1.54118 Å) and a scanning rate of 0.005 deg (2θ/s). Field emission scanning electron microscopy (FESEM) was performed by FESEM, MERLIN with carl ZEISS, SMT, Germany lens and 15 kV accelerating voltage. High resolution transmission microscope (HRTEM) was done by TEM, JEOL, Japan with 24° tilt angle and 200 kV. For the composites, before HRTEM analysis, samples were cut by ultramicrotome at subzero temperature (~70 °C) by Leica with a thickness of around 70 nm. The cut sections were placed in a carbon supported copper grid of 400 mesh. XPS analysis was implemented using Kratos Axis Ultra DLD spectrometer with Al-Kr_α radiation (1486.7 eV). Emission current of the X-ray source was fixed at 20 mA for an anode voltage of 15 kV. XPS samples were prepared by spreading the powder sample on a conducting copper tape. At the same time, Ar^+ beam induced any kind of degradation of the samples has been eliminated by comparing the XPS spectra before and after the sputter cleaning. High resolution XPS spectra were collected using pass energy of 20 eV, with a step size of 0.02 eV. The UHV chamber base pressure was maintained < 10-9 mbar throughout the measurements. To counterbalance any kind of charging effect, O 1s binding energy peak at 532.5 eV has been kept as reference here. The tensile strength of the samples was carried out in a Universal tensile testing machine (Hounsfield H10 KS) at room temperature following the specifications of ASTM D412 and ASTM D624. The crosshead speed was fixed at 500 mm min^{-1}. The tensile were performed in triplicate and taken the average value from the measurements. Thermal properties of the composites were assessed by thermogravimatric analyzer in room temperature to 600 °C (TGA, Shimadzu, Japan) and the differential thermal analysis was performed by DSC Q2000 V24.10 (TA instruments) in the range of -70 °C to 100 °C. Both the thermal characterizations were performed in nitrogen atmosphere with a scan rate of 10 °C/min. Small angle X-ray scattering (SAXS) was performed in Xeuss 2.0, Xenocs, France with an operating voltage of 50 kV and 0.6 mA (30W). The sample to detector (Dectris, Pilatus 300K) distance was 2,500 mm and the q-range was 0.004-0.18 $Å^{-1}$. Silver behenate with 1st order scattering vector of 0.1076 $Å^{-1}$ was used for calibration.

3. Results and discussion

3.1. Morphology and characterizations of silylated graphene oxide (GOF)

Figure 2 is the graphical illustration of the synthesis process of

silane funactionalized graphene oxide (GOF) *via* covalent modification of GO by dichlorodimethylsilane (DCDMS). Visually it can be noticed that the dark brownish GO was transformed into black GOF (Figure 2(a)). The sheet-like morphology of GO and GOF found from the solvent exfoliation technique was evaluated by TEM. The difference between the TEM images of GO and GOF was the wrinkle nature of the sheets (Figure 2(b), (c)) GO showed wrinkled morphology of the sheets whereas GOF have a blackish but smooth type morphology of the sheets. Such darkish nature of GOF sheets can clearly evidence about some deposition on to the sheets.

Surface functionalization of the GO sheets was verified by FTIR shown in Figure 3(a). GO has several characteristic peaks were observed at 1718 cm^{-1}, 1237 cm^{-1} for carbonyl (also -C=O stretching for -COOH) and -C-OH stretching frequency respectively.[38-40] The C-O stretching was observed at 1055 cm^{-1} and the broad absorbance peak was noticed in 3400 cm^{-1} for omnipresent hydroxyl functionalities. The characteristic peaks of aromatic carbon double bonds were seen in 1604 cm^{-1}.[41] The nanocomposites named F1, F4, and F7 in Figure 3(a) revealed that with DCDMS increment, the characteristic peaks of silane become noticeable. The Si-O-CH_3 rocking has the peak at 792 cm^{-1} which became dominant with increasing the silane content from F1 to F7. A very small shoulder appeared around 1081 cm^{-1} in acse of F1 to F7 which is due to the O-C stretching vibration Si-O-C bonds. The shoulder became gradually visible after increase in the DCDMS

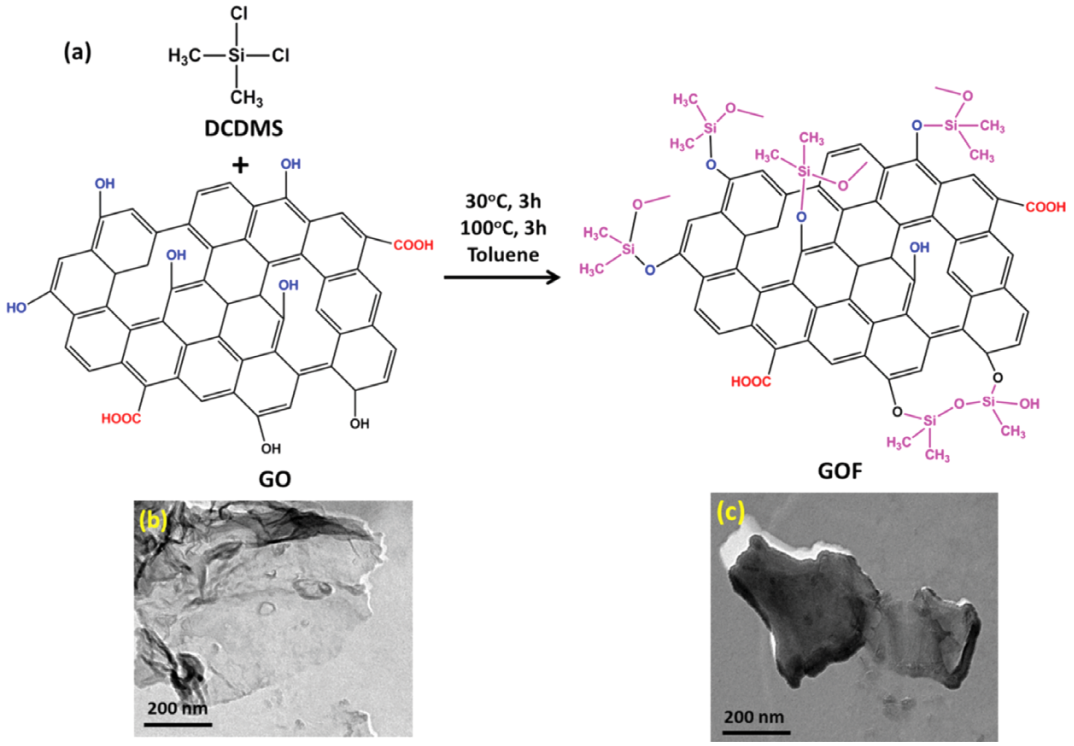

Figure 2. (a) Graphical illustration of silane grafting on GO. TEM micrograph of (b) GO nanosheet and (c) GOF nanosheets.

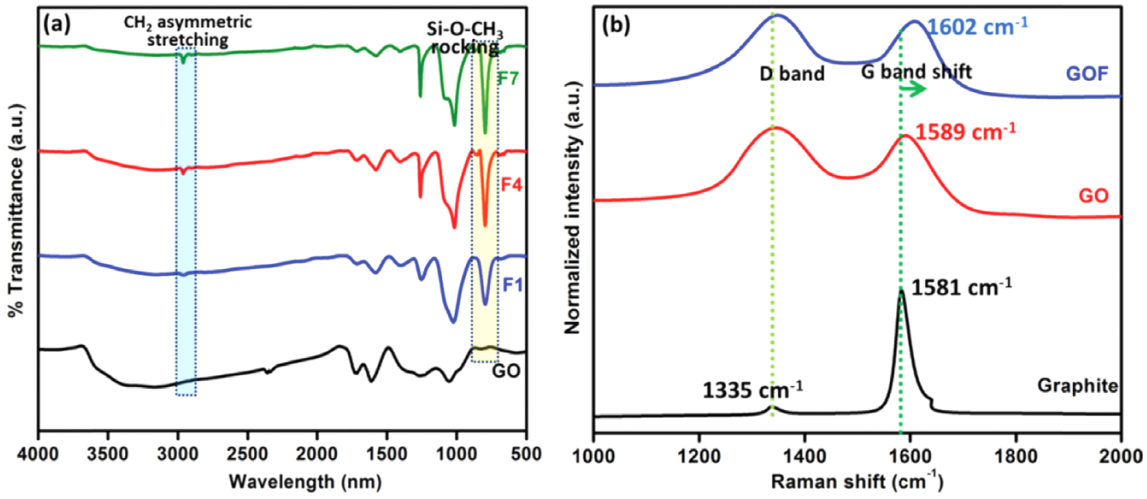

Figure 3. (a) FTIR spectra of GO and DCDMS functionalized GO. (F1, F4, and F7 mean the gradual increment in DCDMS amount during reaction with GO respectively; for better clarification Table 1 formation is helpful) (b) Raman spectra of pristine graphite, GO and functionalized GO (GOF). G peak shift has been shown for GO and GOF with respect to pristine graphine.

content. Another proof of grafting of DCDMS was appearance of asymmetric C-H stretch of -CH_2 groups became prominent in F1, F4, and F7 with increasing their peak intensity. Meanwhile the gradual disappearance of hydroxyl groups (broadened -OH region in GO around 3200-3400 cm^{-1} became flat) in the F1 to F7 also indicates the grafting phenomena.

Figure 3(b) represents the Raman spectra of pristine graphite, GO and GOF. The characteristic peaks at 1335 cm^{-1} (D band) and 1580 cm^{-1} (G band) were noticed for pristine graphite. D and G bands were assigned to the structural defects and first order scattering vibrational of E_{2g} the pristine graphite respectively.[42] It was also been noticed from the figure that there was a right shift of the G band in case of GO and GOF. For GO the peak shifted to 1589 cm^{-1}.[43] GOF showed the G band peak at 1596 cm^{-1} with a broadening. This marked shift of the G band normally implied the partial exfoliation of the graphene layers. Thus it can also be concluded that DCDMS can also acts as an intercalating agent for GO.[44] Furthermore, if the ID/IG ratio was compared with the pristine graphite (0.15), the value increases dramatically for GO (1.19) and GOF (1.22). These values indicate destruction of bonds and symmetry present in the pristine graphite individual basal planes due to reduction of sp^2 domains of graphene sheets by rigorous oxidation.[45]

XPS spectra of GO and GOF were given in given in Figure 4(a). Compared to GO, the XPS spectrum of GOF has two characteristic peaks at Si_{2p} and Si_{2s} originating from DCDMS, which further supports the covalent functionalization of GO by DCDMS. Similar processes were also found in the APTS functionalized graphene.[28,30] The high resolution C1s spectra of GO and GOF in Figure 4(b) and (c) render more evidence. Like the GO, the C1s spectra exhibited a substantial increase for C-C bond (284.6 eV) and the appearance of C-Si bond (283.6 eV) after DCDMS surface covalent functionalization. Here C-Si bond is due to the methyl group and Si covalent linkages. The peak at 283.8 eV corresponds to the C-O-Si peak also which came from the hydroxyl-silane bonding. This bonding is actually the proof of grating of DCDMS to graphene basal plane.

3.2. Exfoliation and dispersion of GOF in EMA matrix

Degree of exfoliation estimation can be determined by XRD analysis of the GOF filled nanocomposites. Figure 5(a)-(e) shows the XRD patterns of pure EMA, pristine graphite, GO, GOF, and GOF filled nanocomposites. Pristine graphite shows a string narrow peak at 27.2° for (002) plane with an interlayer spacing of 0.34 nm. After oxidation the GO shows characteristic peak at 10.8° having a interlayer spacing of 0.89 nm which is similar to other reported results.[42] GOF have a showed an interlayer spacing of 1.16 nm which is clearly evidenced of silane grafting on GO surface which enhances the gallery gap. EMA have characteristic peaks at 21.8° which is due to the crystalline part of ethylene chains present in EMA and another broad peak was observed in 24° because of amorphous part of the EMA. Percentage crytsallinity can be calculated from the following equation:[46]

$$X_c = \frac{I_c}{I_c + I_a} \times 100 \quad (1)$$

where, X_c, I_c, and I_a correspond to the degree of crystallinity

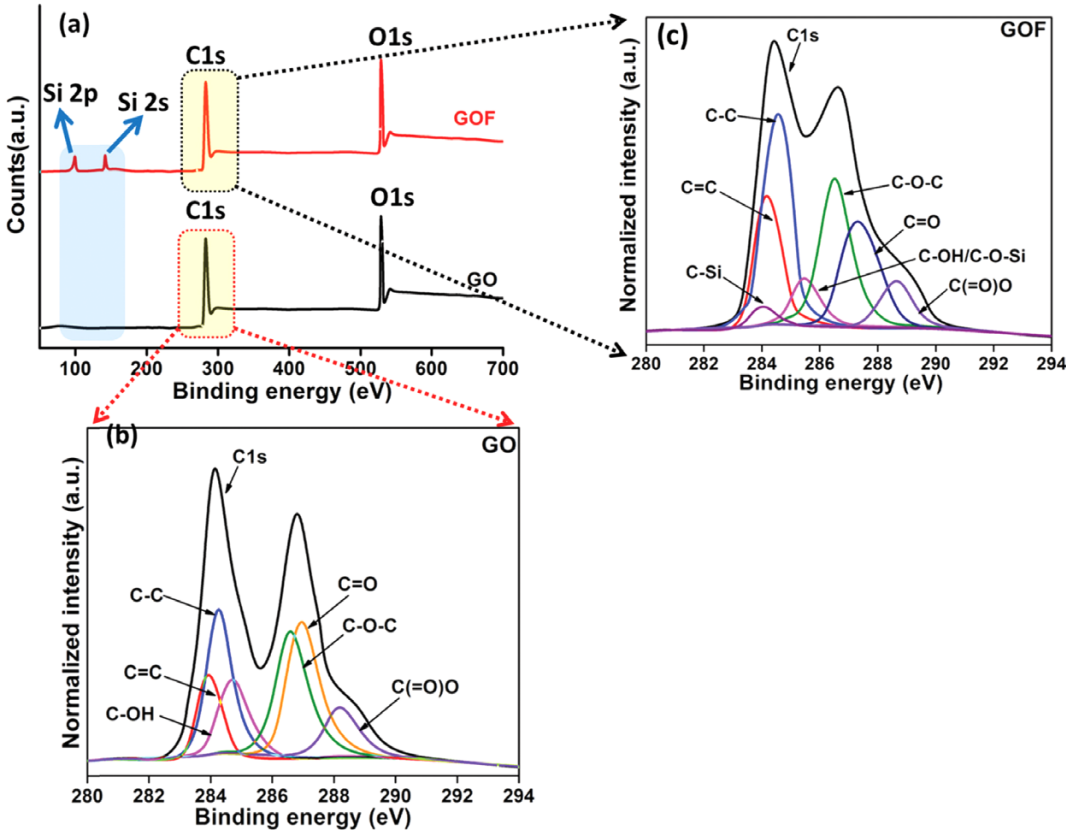

Figure 4. (a) XPS survey scan of GO and GOF; (b) high resolution C1s spectra of GO and (c) high resolution C1s spectra of GOF.

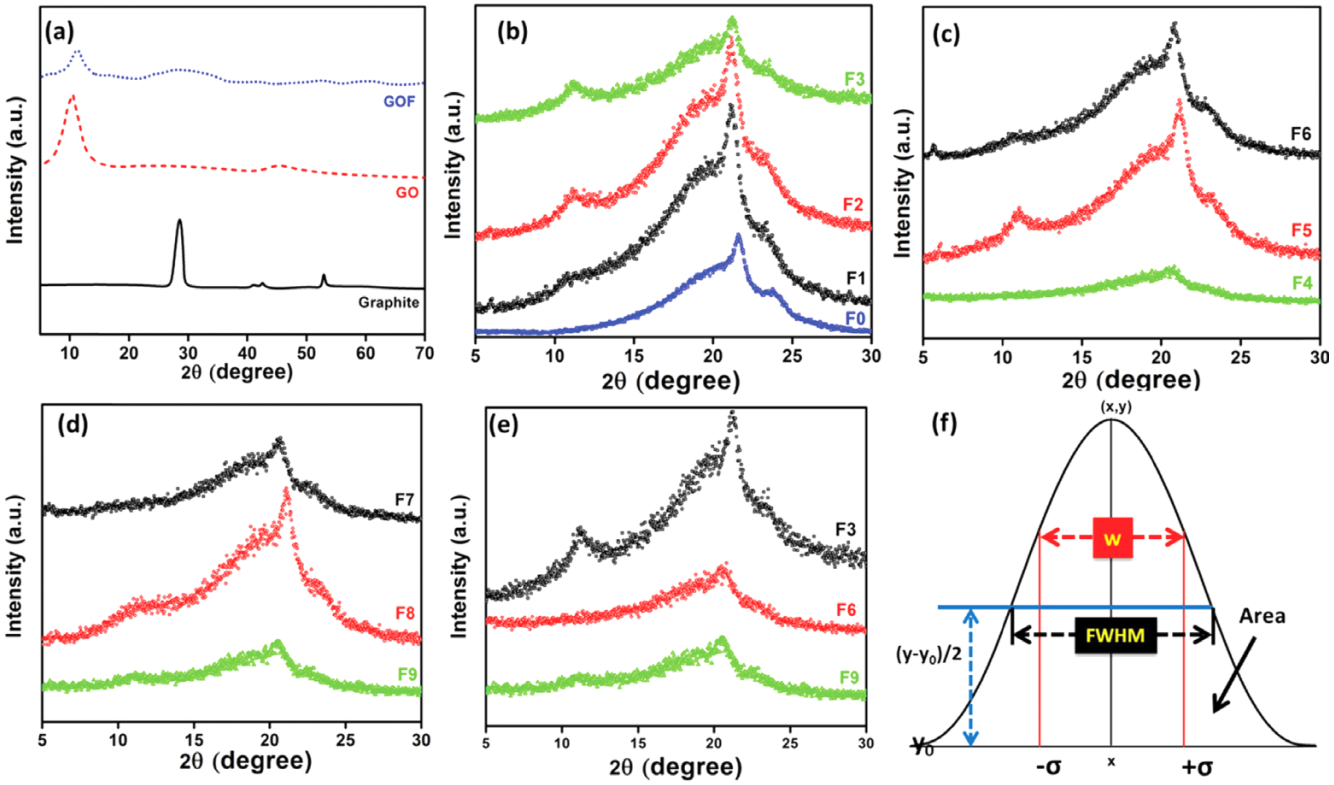

Figure 5. (a-e) XRD plot of pristine graphite, GO, GOF, EMA, and various EMA-GOF composites (F1-F9). (f) Graphical illustration of the Gaussian function used to calculate the area under the fitted curve and FWHM of XRD peaks obtained for different EMA-GOF nanocomposites.

(%), the integrated intensities of crystalline peaks and amorphous peaks of the polymer respectively.

The 2θ values could be reproduced within ±0.02° variation. The crystallite size P (Scherrer equation) was calculated as follows:[47]

$$P = \frac{k\lambda}{\beta\cos\theta} (\lambda = 1{,}542\ \text{Å}) \quad (2)$$

where, β stands for the full width at half-maxima (FWHM) of the crystalline peak, k is the shape factor for the average crystallite (assumed to be 0.9) and λ is the wavelength of the incident X-ray radiation. The area under the curve was computed by Gaussian non-linear curve fitting using the following equation:

$$y = y_0 + \frac{A}{w\sqrt{\pi/2}} e^{-2\frac{(x-x_c)^2}{w^2}} \quad (3)$$

Here, A is the area under the curve, x_c is the x co-ordinate at the centroid and w is the peak width and can be calculated as w= 2σ; where σ is the standard error of the Gaussian distribution curve. For betterment of understanding a graphical illustration was shown in Figure 5(f). The calculated parameters obtained from diffractograms are given in Table 2. The fluctuation of the characteristic peaks of EMA was changed after incorporation of GOF was observed. This change in peaks was may be due to the structural disturbances in the crystalline domains of EMA after addition of GOF.[48] A drastic drop in the crystallite size was noticed according to Table 2 due to addition of GOF nanoparticles in the EMA matrix. This drastic drop in crystallite size probably a result of higher lattice strain stimulated after introduction of another heterophase (here GOF particles). During mixing and sonication the GOF could interact with the crystalline domains of EMA (ethylene domains) and the there was a fair chance of

Table 2. Structural parameters of neat EMA and F1 to F9 nanocomposites obtained from XRD

Code	Crystallite size (P1)	Crystallite size (P2)	Crystal size anisotropy (P1/P2)	Degree of crystallinity (%)
EMA	5.04	7.03	0.716	31.66
F1	4.96	6.57	0.755	31.15
F2	4.94	5.89	0.83	30.56
F3	4.91	5.12	0.959	29.22
F4	4.93	6.41	0.769	30.58
F5	4.88	5.33	0.915	30.11
F6	4.76	4.33	1.099	29.14
F7	4.72	6.02	0.784	28.47
F8	4.61	4.88	0.944	26.05
F9	4.52	4.02	1.124	24.15

crystallinity destruction resulting lowering of crystallite domain size decrement.[49] This lowering of crystallinity was also noticed after observing the peak broadening and lowering of intensity of the characteristic peak of EMA. Such rupturing the crystalline domains normally deteriorates the mechanical properties of the composites, but the stress transfer phenomena was more dominant factor here to withstand the external applied stress. Thus the mechanical strength was also enhanced which is discussed later in 'mechanical property' section.

3.3. SAXS analysis

The reinforcing activity of GOF nanoparticles in polymer matrix was established by virtue of SAXS analysis of the composites as shown in Figure 6. Polymer chains are very prone to adsorbed onto the surface of graphene sheets by virtue of their surface energy which can be termed as physorption. Now the point of discussion is how this reinforcing activity can be justified in the light of scattering. For a disordered system the microstructure can be named as self-similar domains/portions present in matrix which is called fractals. These fractals are the outcomes of GOF sheets-polymer adhered portions which normally increase with filler loading. Thus to evaluate these fractals and hypothesize the microstructural array inside the polymer matrix unified approach has been implemented.[50-52] Figure 7 shows the data fittings in unified power law model. The power law based on scattering data can be described as follows,

$$I(q) \cong q^{-p} \tag{4}$$

where $I(q)$, q and p denote the scattering intensity, scattering vector and power law exponent respectively. This power law was modified by Beaucage based on microstructure and aggregates of the fillers inside the matrix which is shown below,

$$I(q) \sim G \exp\left(\frac{-q^2 R_g^2}{3}\right) + B\left[\frac{(erf(qR_g/\sqrt{6}))^3}{q}\right]^p \tag{4a}$$

Here G is the classic Guinier pre-factor and B is a power law specific pre-factor. 'q' stands for scattering vector. The value of

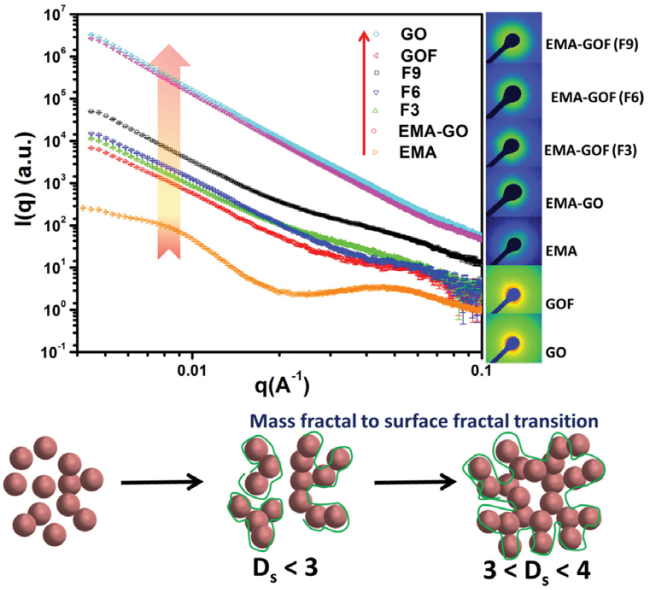

Figure 6. Scattering intersity versus scattering vactor plot for pure EMA, EMA-GO and other nanocomposites (below: graphical illustration of fractal dimension).

p lies between 3 and 4 for surface fractals whereas, for mass fractals the value lies below 3. The value less than 3 corresponds to the surface irregularities and asperities. If p value lies in between 3 and 4, then the particles are taken into consideration as surface fractals (D_s). The relation between D_s and p is p=6-D_s. Now, it can be stated that, 3<(6-D_s)≤4. The calculated surface fractals for GO and GOF were 2.211 and 2.15. The D_s values of GO was calculated to be higher than GOF due to their higher surface energy. In case of the composites, the D_s values were 2.72, 2.73, and 2.81 for F3, F6 and F9, respectively. High surface fractals correspond to the high radius of gyration for the particulate materials inside polymer matrix. Polymer chains are physically adsorbed over the GOF nano-sheets resulting increment in radius of gyration. But here negligible increment on D_s values corresponds to the negligible alteration of radius of gyration. This means effective dispersion of filler inside thermoplastic matrix. But in case of our previously prepared EMA/GO system the radius of gyra-

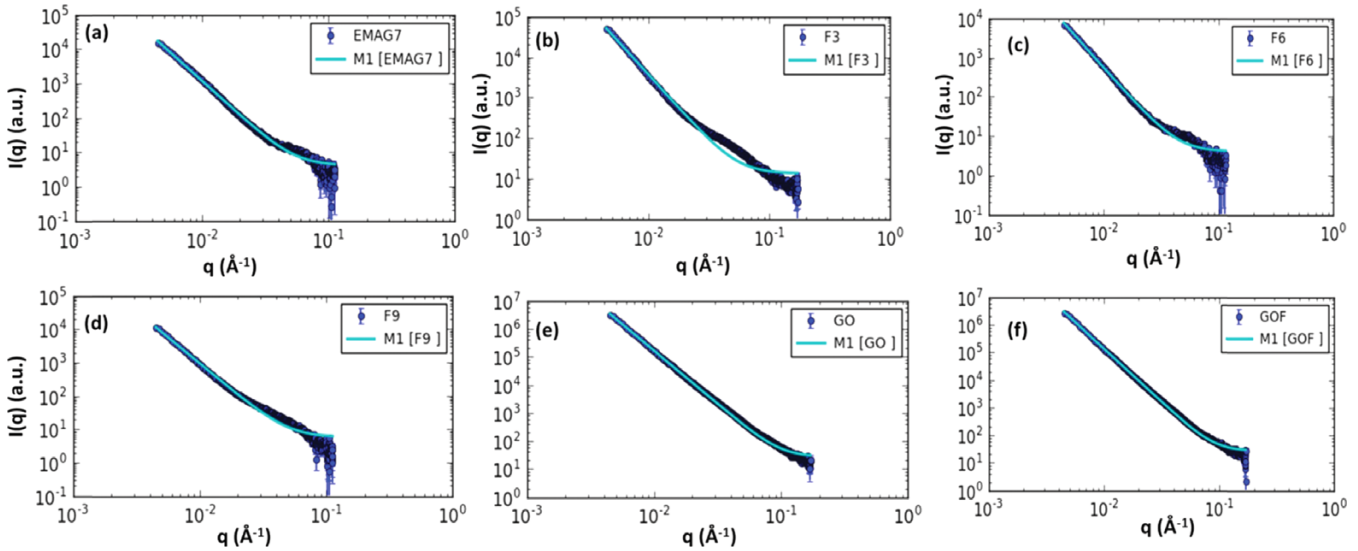

Figure 7. SAXS intensity *vs.* scattering plot after data fitting in power law model. The cyan coloured line represents the fitting line.

tion was comparatively high due to the inter-filler agglomeration.[36] Being a high surface energy filler, GO has tendency to cohere as a self-assembly; nonetheless, the polymer chains were also adhered with GO exposed surfaces. This could be hypothetically attributed that silylated GO (*i.e.* silane grafted GO) is better replacement instead of unmodified GO.

3.4. Mechanical property

Mechanical property of the composites was estimated by their tensile property analysis. According to Figure 8(a)-(d) it is clearly seen that with increasing the GOF, the tensile strength increases which means GOF has an obvious reinforcing effect. In our previous work it was noticed that GO have not so much of reinforcement on EMA matrix due to their high chance of self-agglomeration and high aspect ratio. In case of GOF, the surface energy was enhanced by covalent grafting reaction which makes GOF dispersible in EMA matrix. In case of GO the tensile was not much improved than GOF loaded nanocomposites. According to FTIR spectra it was noticed that covalent functionalization was successful which resulted silane grafted GO or GOF. The total scenario of dispersion of GOF fillers and intercalation has been

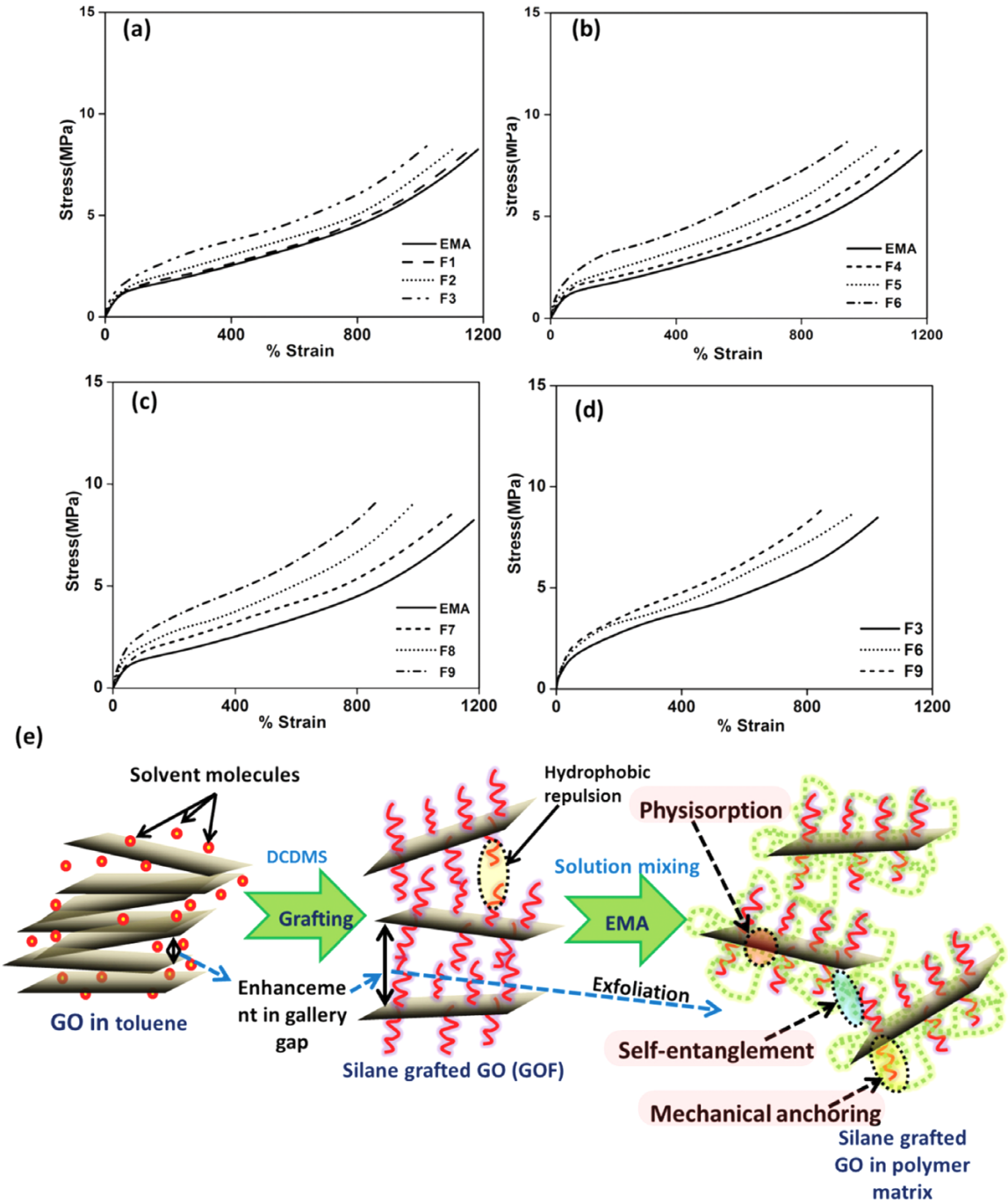

Figure 8. (a-d) Stress-strain plots of all composites (comparing pristine EMA with others). (e) Mechanism of exfoliated GO sheets and gafting with DCDMS molecules. Grafting on to GO surface enhance the inter-sheets spacing which is quite desiable for further intercalation/exfoliation during polymer mixing. DCDMS functionalized nanosheets have three plausible interaction approach with EMA which is also shown here.

illustrated pictorially in Figure 8(e). These GOF nanosheets have higher gallery gap than GO which is accepted for intercalation of nanosheets. Intercalated nanosheets can act as stress transfer center for a composite. At the time of mixing the EMA chains have sufficient proneness to get attached onto the GOF surface by means of physisorption. The physisorped chains can act as a physical crosslinking site in the nanocomposite matrix. Such nanosheet-polymer chain adhered domains can be termed as 'fix points' which is the stress transfer points. GO, because of their high polarity and surface charge are very much prone to agglomerate in polymer matrix. Such kind of phenomenon was also a known phenomenon for carbon-black filled rubber composites.[53] Due to the high compatibility of GOF in EMA matrix, there might be sufficient interfacial interactions between GOF and EMA polymer chains which can improve the mechanical property by stress transfer phenomenon. When external load is applied in a polymer nanocomposite, the elastic phase (GOF) becomes much responsive to bear the stress which was transferred to the viscoelastic polymer phase. If the graphene sheets are much dispersed in polymer matrix, the nanocomposite will sustain more loads. In case of GO, the high surface tension was liable for their better dispersion in polymer matrix, thus sufficient stress transfer was not implemented. In case of GOF, there was an increase in 'fix points' which have an obvious effect of stress transfer phenomena which results the better load bearing capability of the composites. Generally high loading of GO suffers from lack of dispersibility as well inferior mechanical property. This can be avoided by means of the GOF insertion which has a compatibilization effect with EMA used. For high loading of GOF with respect to the GO, does not seem to such adverse effect of agglomeration as of our experimentation. With higher amount of silane grafting, the mechanical property enhanced surprisingly which has a resemblance to other research works.[9,30,54] The detailed data regarding the stress-strain experiment of the nanocomposites has been tabulated in Table 3.

Figure 9 is the SEM images of unfilled EMA and GOF filled EMA composites. SEM was performed after etching in chloroform. Figure 9(a) showed smooth surface of EMA. After 3 wt% loading (F2), the functionalized graphene sheets were clearly visible after solvent etching (Figure 9(b)). Graphene sheets were stacked together which was seen in Figure 9(c). For better understanding of the bulk property of the GOF filled nanocomposites, F2 specimen was cryofractured after uniaxial tension. It was observed that for 3 wt% GOF loaded EMA composite showed uneven surface roughness which was due to the physical attachment of graphene platelets and the EMA macromolecular chains. This means graphene sheets had good adhesion with the polymer chains by virtue of physisorption as described in mechanical property enhancement. Surprisingly after addition of much amount DCDMS, the functionalized graphene sheets (GOF) become more effective to get anchored with EMA sheets. The surface roughness was became little bit smoother for F8 with respect to the F2 specimen. It also helped to establish that silaylation on to graphene basal plane might improve the compatibility as well as better reinforcing character of graphene fillers. Similar kind of results also have been reported elsewhere.[55]

3.5. Dynamic mechanical property of EMA-GOF composites

The viscoelastic response of polymer and its composites was assessed by dynamic mechanical analysis (DMA) which was depicted in Figure 10(a). The study was done in a temperature range of -80 °C to +80 °C and plotted the elastic modulus versus temperature (°C). Elastic modulus or storage modulus is an amount of retrievable strain energy in a deformed composite which reflects basically the elasticity of the composite. Loss factor (tan δ) is another parameter associated to the damping characteristics of the same composite. Figure 10(a) shows the trend of storage modulus after altering the temperature in a specific rate. It is seen that the storage modulus increased after incorporation of the GOF filler into the EMA matrix. After silane modification the enhancement in storage modulus was surprisingly high. GOF being compatible due in EMA matrix, the stress transfer phenomenon become more prominent for the prepared composites. When temperature increased the physisorped polymer chains on GOF surface were hindered to flow which was totally absent in case of pristine EMA. When GO was functionalized with some organic groups, the GO surface become very much rough. The surface roughness of the GOF nanosheets likely resulted rising of mechanical properties and as an obvious effect the polymer chains were unable to 'plastic flow' or better to express as adhesion between GOF and EMA chains. Similar kind of study was reported elsewhere.[56,57] This can increase the storage modulus value of the composites. This increment in storage modulus is

Table 3. Mechanical properties of GOF filled EMA nanocomposites

Code	TS (MPa)[a]	TS increment	EB (%)[b]	M@100%[c]	M@200%	M@300%
F0	8.1	-	1185	1.8	2.1	2.3
F1	8.2	2.5	1146	1.9	2.3	2.6
F2	8.2	2.5	1103	1.9	2.4	2.6
F3	8.4	5.0	1021	2.2	2.8	3.4
F4	8.2	2.5	1111	2.0	2.5	2.9
F5	8.4	5.0	1038	2.3	2.9	3.5
F6	8.7	8.75	946	2.6	3.4	4.1
F7	8.5	6.25	1110	2.2	2.5	3.4
F8	8.8	11.25	982	2.6	3.6	4.1
F9	9.2	15.0	860	3.1	4.2	4.9

[a]Tensile strength. [b]Elongation at break. [c]Modulus at X% elongation.

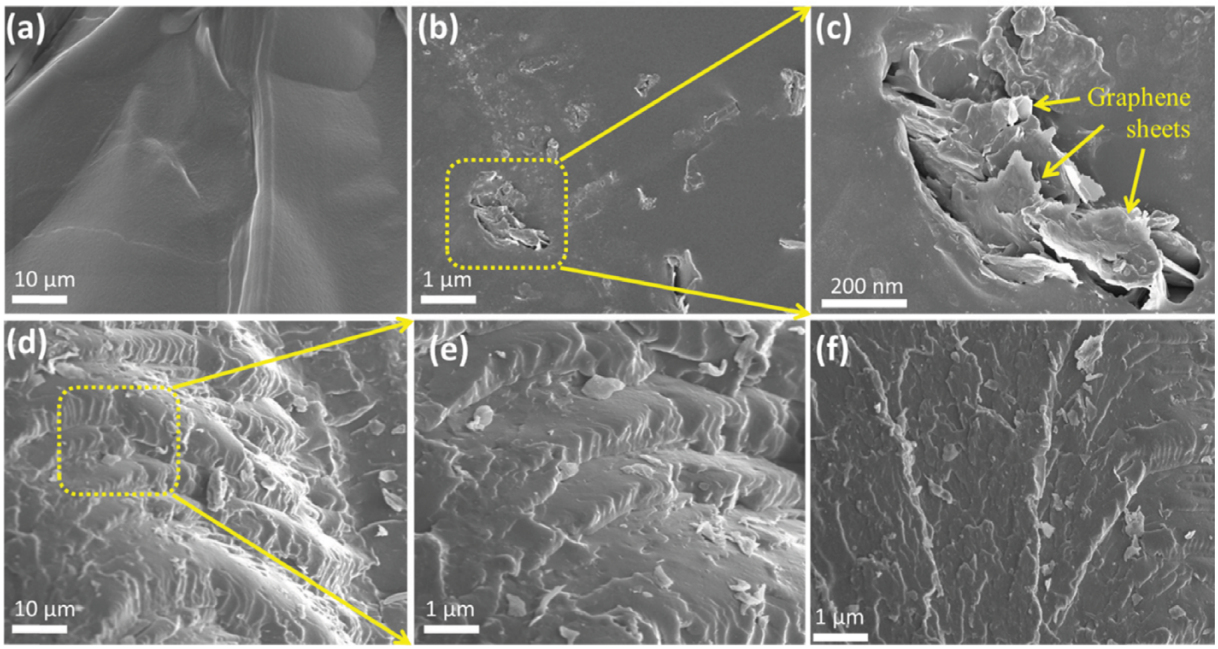

Figure 9. FESEM images of (a) Prinstine EMA and (b) 3 wt% GOF filled (F2) nanocomposite. (c) Magnified image of the graphene sheets after surface itching. Sheets are stratified inside the EMA matrix (d) tensile cryofacture surface of 3 wt% GOF filled (F2) specimen (e) magnified F2 of selective area shows surface roughness (f) cryofactured surface of F8 (3 wt% GOF filled) sample shows better surface smoothness than F2 corresponds to the better compatibilization after silylation of GO.

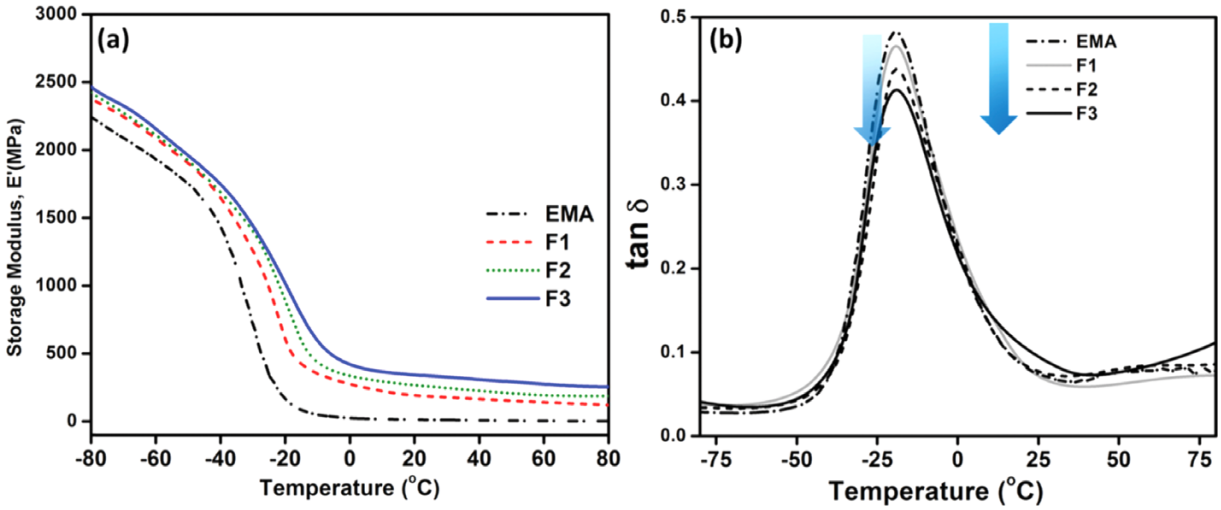

Figure 10. (a) Dynamic storage modulus and (b) damping factor (tan δ) as a function of temperature for neat EMA, F1, F2, and F3 nanocomposites.

going high with the silane content; that intends more the grafting more will be the storage modulus. This also implies the higher stiffness of the GOF filled composites than the pure EMA. The damping character was revealed in Figure 10(b). In case of pure EMA, the tan δ showed a sharp peak. With filler loading, the peak becomes smaller. The lowering of the peak height implied the enhancement of storage modulus. The peak shift was also seen in case of the high loaded nanocomposites. Shifting of tan δ towards high temperature means enhancement of physical interaction between filler and polymer chains which corresponds to effective interfacial adhesion between polymer phase and GOF. Functionalized graphene sheets have similar type possibility in acrylate polymer matrix which also has been reported earlier.[58]

3.6. Thermal property analysis

Thermogravimetric characterization of pristine graphite, GO, GOF and other GOF filled composites were given in Figure 11(a). In Figure 11(a) the comparison among the pristine graphite, GO and GOF was given. Pristine graphite showed no abrupt change in mass loss up to 700 °C. But after oxidation to GO, it showed decomposition at approx. 250 °C which is assumed to be the pyrolysis of the oxygenated functionalities (like -OH, -COOH, -C=O, *etc.*). These oxygenated functionalities generally evolve carbon monoxide, carbon dioxide and vapour during heating.[59] If we compare GOF with GO, it can be clearly seen that GOF has better thermal stability than GO. This trend can be reflected from the fact of delayed degradation of Si-O-Si bond formed

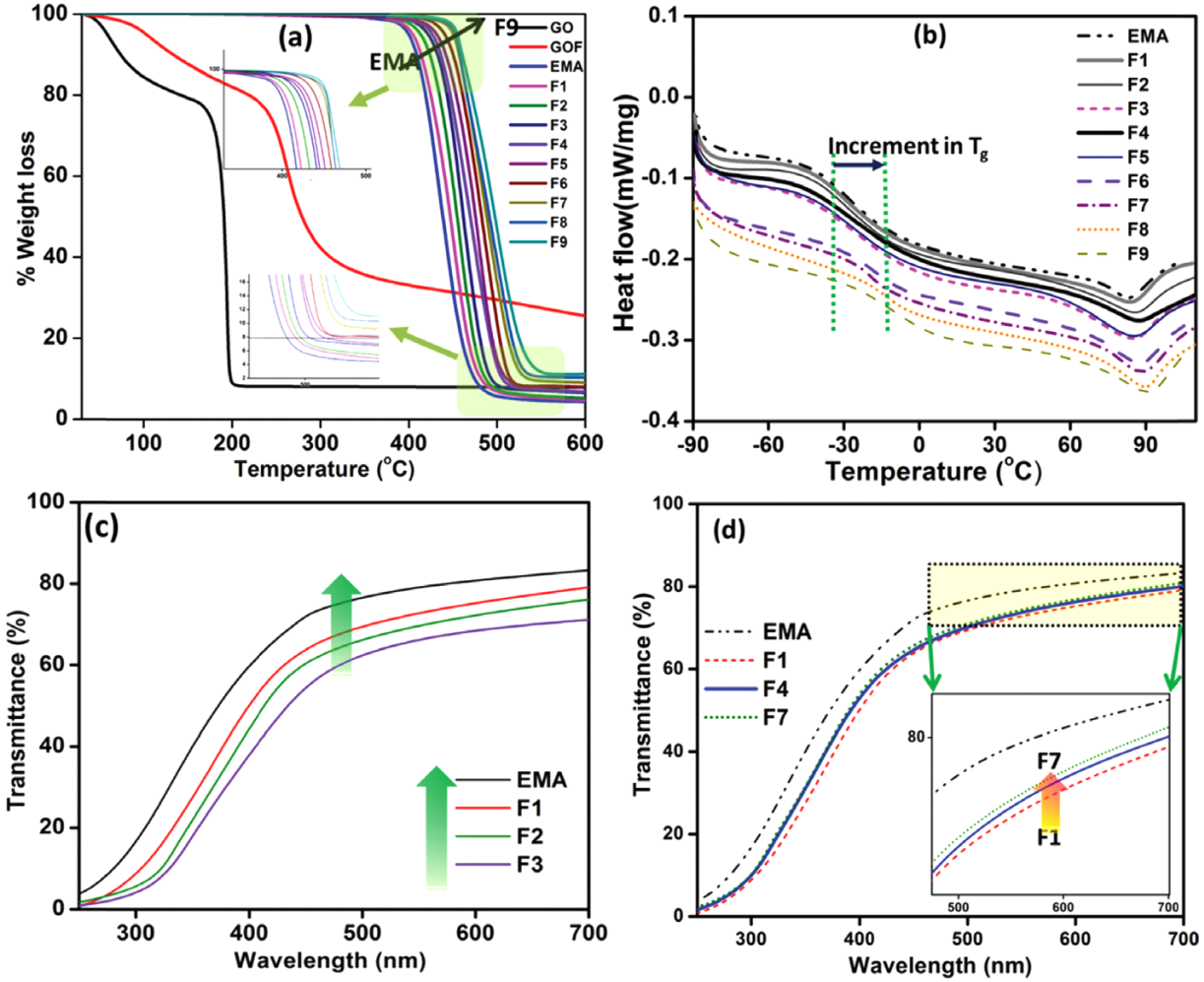

Figure 11. (a) TGA plot of GO, GOF, pure EMA, and other GOF filled composites (F1 to F9). (b) DSC thermogram of pure EMA and other EMA-GOF composites. Increasing the GOF filler enhances the T_g. UV-Visible spectra of pristine EMA and GOF filled EMA nanocomposites. All films are molded around 0.2 mm thickness with loading variation (c) and silane variation (d).

during grafting reaction. This can be also a proof for silylation on GO surface.

For composites, it is very obvious that incorporation of filler normally enhances the thermal stability. Figure 11(a) also shows the comparative thermal stability of the GOF filled composites. In Figure 11(a) the thermal stability of the composites gradually increases with GOF loading from F0 to F3. This improvement in thermal stability was also seen in the Figure 11(a). As per the Figure 11(a) it is seen that DCDMS have significant effect in improving the thermal stability. The samples of F3, F6, and F9 were tallied on account of their DCDMS content. With increasing DCDMS content the GO may subjected to graft rigorously. These grafting can efficiently compatibilize the GOF in EMA matrix. DCDMS generally impose hydrocarbon substituents in the GO basal planes. Thus results minimizing the surface energy of GO and prevents them to agglomerate even in EMA matrix. More the delocalization of the GOF sheets in the matrix more will be the thermal stability because of their heat dissipation. But in case of GO, there was improper distribution of the GO sheets in the thermoplastic matrix which evolves localized heat generation in the polymer composites; thus gradual degradation was inevitable with respect to the GOF filled EMA matrix. The onset of degradation was also found to be shifted almost 13 °C with increasing the DCDMS content. Such trend has also been reflected in their mechanical properties.

Differential scanning calorimetry (DSC) gives the idea of glass transition temperature (T_g) of the composites prepared. T_g gives the idea of molecular chain relaxation behaviour after addition of GOF. The DSC thermograms of different composites were given in Figure 11(b). The plot shows that with addition of GOF in EMA matrix, the T_g increases. EMA has a T_g of -34 °C which was right shifted in plot with gradual GOF loading. The melting peak (T_m) of pure was also increased after addition of GOF. The rigid nanofiller basically restricts the chain movement, as a result the T_g and T_m both increases gradually. The effect of compatibization of GOF nanoparticles with the EMA matrix enhanced the adsorption of polymer chains on to GOF surface which is also another plausible cause for chain restriction in the GOF filled nanocomposites.

3.7. Transparency of the nanocomposite films

Figure 11(c) is the % transmittance plot of the pristine EMA and GOF filled nanocomposite films. According to Figure 11(c)

it is clear that with increasing the filler content the transparency gradually diminished. In higher loading of fillers, the light wave was hindered by the dispersed fillers in the polymer matrix, thus decreasing in transparency was noticed. In Figure 11(d), one interesting finding has been noticed. For same loading of DCDMS functionalized GO in the EMA matrix, the degree of transparency is proportional to the silane addition. DCMDS grafted on to the GO basal planes which may serve dual purposes; compatibilization with polymer phase and exfoliation of GOF nanosheets in matrix. The results revealed that with increasing the silane content, the compatibility increased, thus nanofiller dispersion was effective in that case. Hence, as a matter of fact the transparency can be correlated to the filler dispersion in polymer matrix. Superior dispersion or filler compatibility makes the nanocomposite transparent and this filler dispersion also improved the mechanical properties which have been already discussed in mechanical properties section.

3.8. Proposed mechanistic pathway of DCDMS grafting over GO surface

The primary requirement to couple GO and polymer matrices is to choose a silane molecule with atleast bifunctional groups. Bifunctionlaity is effectively liable to form a bridge between poly-

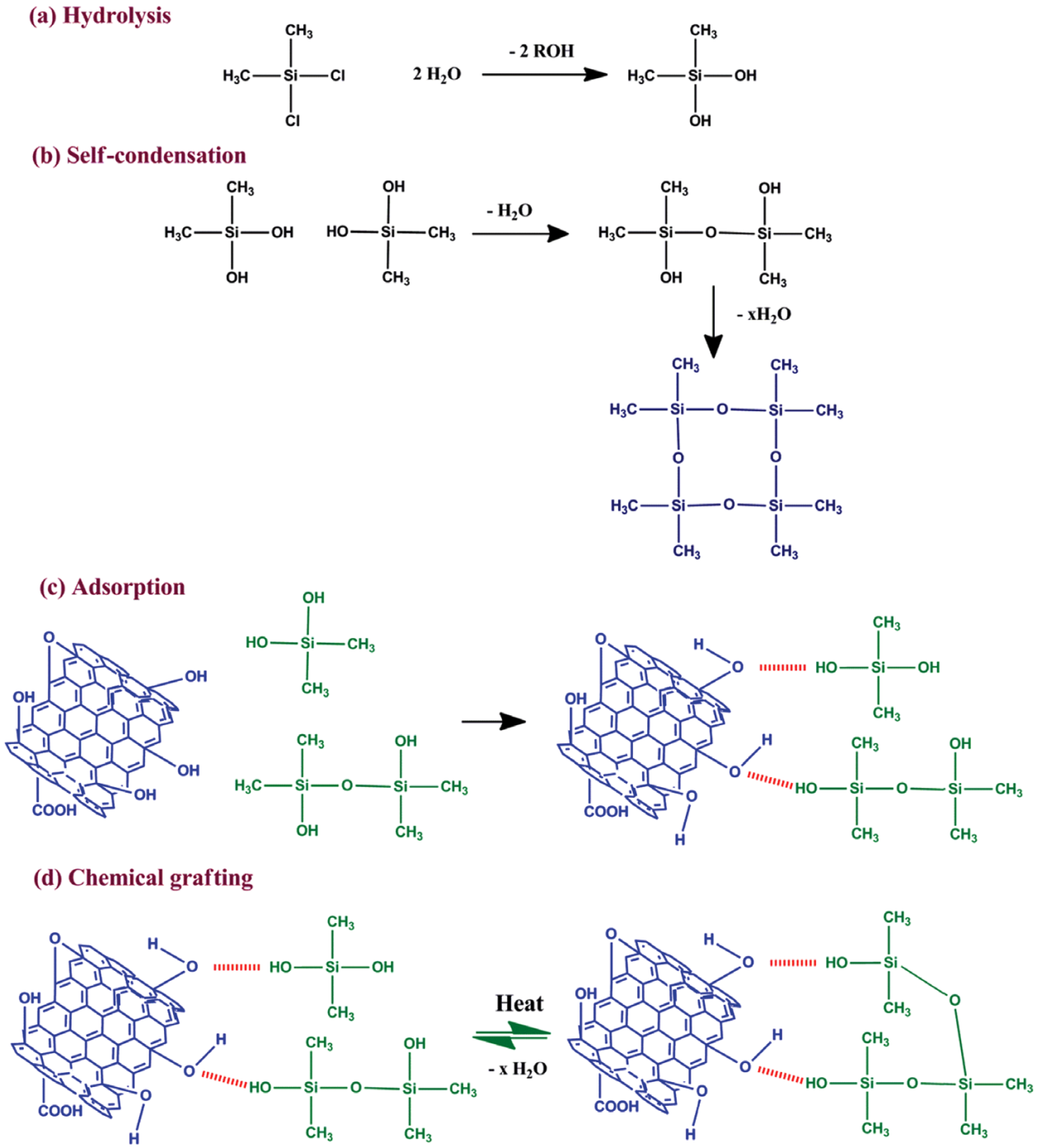

Figure 12. Schematic representation of the proposed mechanism for grafting.

mer matrices and GO. In general GO have high aspect ratio and high polarity which is a major problem for dispersion into a polymer matrix having moderate to lower polarity. Lack of dispersion of filler into polymer matrix deteriorates the mechanical property and early failure of composites. Most of the silanes impose organic functionality and oleophilicity into the fillers which enhances interaction as well as compatibility with the polymer. A non-reacting hydrocarbon (alkyl groups) side group present in silane may increase the properties of nanocomposites synergistically. Among the organic modifications, covalent functionalization has been chosen to improve the thermo-mechanical attributes of the nanocomposites.

The basis of the silane functionalization is terminologically said as hydrolysis process. Herein we used DCDMS as the silane coupling agent which has two chloro and two alkyl (methyl) groups. The surface hydroxyl groups of GO were very much prone to react with DCDMS followed by evaluation of hydrochloric acid fume. The pungent smell during hydrolysis is also a proof of silylation reaction. The hydrolysis process forms Si-O-C bond as a grafting to GO surface. The silylation follows some generic reactions which can be classified as (a) hydrolysis, (b) self-condensation, (c) adsorption and (d) chemical grafting. The stepwise illustration has been schematically produced in Figure 12. Initially when silanes are added into the water-ethanol solution, hydrolysis has been occurred resulting evolution of alcohol and produce reactive silanol groups in the medium. These silanols can further condense to produce -Si-O-Si- three dimensional networks. This step is known as 'self-condensation' process. In this process the hydroxyl functionalities of the GO get attached to the silanol groups by adsorption. This adsorption of silanols onto GO surfaces was carried forward to silylation. The small molecular size of DCDMS can diffuse into the GO stacked arrangements and generates the polysiloxane type coating/grafting over GO nano-surfaces. The typical polysiloxane bonding *i.e.* -Si-O-Si- has high thermal stability which imposes better thermal properties of the GOF loaded composites.

After proper silanol grafting on GO surfaces, the inherent hydrophillicity of the GO became diminished, thus hydrophobation of GO was imposed. Hydrophobation can show self-stabilization effect of silane functionalized GO in polar environment by avoiding agglomeration or restacking. The intermolecular H-bonding present in GO was weakened after silane grafting. Thus the weakening of H-bonding increases the 'gallery gap' between inter-platelets of GO. Enhancement in the gallery gap is very much desirable for p high degree of intercalation/exfoliation of nanofiller (here GOF) into the polymer matrix (here EMA). Thus GOF nanofiller has very little water sorption rate which prevent the loosely bound moisture in the GOF surface.[60] Loosely bound surface moisture affects deterioration of composites in its service life by blistering.

4. Conclusions

In this work, the silylation over GO was implemented followed by wet mixing of the as-prepared material as reinforcement in polymer matrix. The significant findings obtained from the work are summed up as follows: (a) dispersion of silane functionalized GO has a major dominance over un-modified GO in respect to the extent of filler dispersion in polymer matrix; (b) uniaxial tensile strength was improved for GOF filler with respect to GO filler which was hypothesized as the surface compatibility and enhanced physisorption of polymer chains onto GOF basal planes; (c) lyophilic modification of GO surface also enhanced the transparency of nanocomposites and as a result the thermal stability; (d) most surprisingly it is work mentioning that the all aforementioned attributes were overcome without comprising the glass transition temperature (T_g) drastically. This implied keeping their softness even at moderate loading (5 wt%) of GOF as filler. Besides these, the SAXS study was executed for all composites which corroborated the dispersion overview of GOF inside polymer (EMA) matrix. The negligible enhancement in radius of gyration has been observed which provides information of 'not-to-cohere' tendency of GOF particles in matrix. Inter-filler interaction is a major component for premature failure of composite on service. For GOF reinforced polymer nanocomposites, filler-polymer interaction was a dominant factor whereas for GO reinforced polymer (EMA) the inter-filler interaction was noticed as a recessive factor. Hence, it can be concluded that, silylated GO has a prominent effect of reinforcement in polymer matrix over pure GO; provided the polymer should have lack of polarity.

References

(1) K. Novoselov and A. Geim, *Nat. Mater.*, **6**, 183 (2007).
(2) S. Stankovich, D. A. Dikin, G. H. Dommett, K. M. Kohlhaas, E. J. Zimney, E. A. Stach, R. D. Piner, S. T. Nguyen, and R. S. Ruoff, *Nature*, **442**, 282 (2006).
(3) L.-C. Tang, X. Wang, L.-X. Gong, K. Peng, L. Zhao, Q. Chen, L.-B. Wu, J.-X. Jiang, and G.-Q. Lai, *Compos. Sci. Technol.*, **91**, 63 (2014).
(4) S. Ganguly, D. Ray, P. Das, P. P. Maity, S. Mondal, V. Aswal, S. Dhara, and N. C. Das, *Ultrason. Sonochem.*, **42**, 212 (2018).
(5) M. A. Rafiee, J. Rafiee, I. Srivastava, Z. Wang, H. Song, Z. Z. Yu, and N. Koratkar, *Small*, **6**, 179 (2010).
(6) L. He and S. C. Tjong, *Nanoscale Res. Lett.*, **8**, 1 (2013).
(7) M. Monti, M. Rallini, D. Puglia, L. Peponi, L. Torre, and J. Kenny, *Compos. Part A: Appl. Sci. Manufacturing*, **46**, 166 (2013).
(8) S. Chandrasekaran, G. Faiella, L. Prado, F. Tölle, R. Mülhaupt, and K. Schulte, *Compos. Part A: Appl. Sci. Manufacturing*, **49**, 51 (2013).
(9) Y.-J. Wan, L.-X. Gong, L.-C. Tang, L.-B. Wu, and J.-X. Jiang, *Compos. Part A: Appl. Sci. Manufacturing*, **64**, 79 (2014).
(10) X. Yang, Y. Zhang, Y. Xu, S. Gao, and S. Guo, *Macromol. Res.*, **25**, 270 (2017).
(11) P. Bhawal, S. Ganguly, T. K. Das, S. Mondal, S. Choudhury, and N. Das, *Compos. Part B: Eng.*, **134**, 46 (2018).
(12) P. Bhawal, T. K. Das, S. Ganguly, S. Mondal, R. Ravindren, and N. Das, *J. Polym. Sci. Appl.*, 2018 (2017).
(13) M. J. McAllister, J.-L. Li, D. H. Adamson, H. C. Schniepp, A. A. Abdala, J. Liu, M. Herrera-Alonso, D. L. Milius, R. Car, and R. K. Prud'homme, *Chem. Mater.*, **19**, 4396 (2007).
(14) A. Malas and C. K. Das, *Compos. Part B: Eng.*, **79**, 639 (2015).
(15) N. T. Tung, T. Van Khai, M. Jeon, Y. J. Lee, H. Chung, J.-H. Bang, and D. Sohn, *Macromol. Res.*, **19**, 203 (2011).
(16) B. Shen, W. Zhai, M. Tao, D. Lu, and W. Zheng, *Compos. Sci. Technol.*, **77**, 87 (2013).
(17) M. E. Uddin, R. K. Layek, N. H. Kim, D. Hui, and J. H. Lee, *Compos. Part B: Eng.*, **80**, 238 (2015).

(18) S. Ghosh, S. Remanan, S. Mondal, S. Ganguly, P. Das, N. Singha, and N. C. Das, *Chem. Eng. J.*, **344**, 138 (2018).
(19) D. R. Bortz, E. G. Heras, and I. Martin-Gullon, *Macromolecules*, **45**, 238 (2011).
(20) M. Fang, Z. Zhang, J. Li, H. Zhang, H. Lu, and Y. Yang, *J. Mater. Chem.*, **20**, 9635 (2010).
(21) C. Bao, Y. Guo, L. Song, Y. Kan, X. Qian, and Y. Hu, *J. Mater. Chem.*, **21**, 13290 (2011).
(22) M. Cano, U. Khan, T. Sainsbury, A. O'Neill, Z. Wang, I. T. McGovern, W. K. Maser, A. M. Benito, and J. N. Coleman, *Carbon*, **52**, 363 (2013).
(23) S. Ganguly and N. C. Das, in *Flexible and Stretchable Electronic Composites*, Springer, 2016, pp 229-259.
(24) S. Ganguly, P. Bhawal, R. Ravindren, and N. C. Das, *J. Nanosci. Nanotechnol.*, **18**, 7641 (2018).
(25) W.-S. Ma, J. Li, and X.-S. Zhao, *J. Mater. Sci.*, **48**, 5287 (2013).
(26) S. Hou, S. Su, M. L. Kasner, P. Shah, K. Patel, and C. J. Madarang, *Chem. Phys. Lett.*, **501**, 68 (2010).
(27) Z. Li, R. Wang, R. J. Young, L. Deng, F. Yang, L. Hao, W. Jiao, and W. Liu, *Polymer*, **54**, 6437 (2013).
(28) H. Yang, F. Li, C. Shan, D. Han, Q. Zhang, L. Niu, and A. Ivaska, *J. Mater. Chem.*, **19**, 4632 (2009).
(29) Y. Lin, G. J. Ehlert, C. Bukowsky, and H. A. Sodano, *ACS Appl. Mater. Interfaces*, **3**, 2200 (2011).
(30) X. Wang, W. Xing, P. Zhang, L. Song, H. Yang, and Y. Hu, *Compos. Sci. Technol.*, **72**, 737 (2012).
(31) S.-Y. Yang, W.-N. Lin, Y.-L. Huang, H.-W. Tien, J.-Y. Wang, C.-C. M. Ma, S.-M. Li, and Y.-S. Wang, *Carbon*, **49**, 793 (2011).
(32) D. Vennerberg, Z. Rueger, and M. R. Kessler, *Polymer*, **55**, 1854 (2014).
(33) P. Bhagabati and T. Chaki, *J. Appl. Polym. Sci.*, **131** (2014).
(34) S. Ganguly, P. Bhawal, A. Choudhury, S. Mondal, P. Das, and N. C. Das, *Polymer-Plastics Technol. Eng.*, **57**, 997 (2018).
(35) P. Bhawal, S. Ganguly, T. K. Das, S. Mondal, and N. Das, *Polym. Adv. Technol.*, **29**, 95 (2018).
(36) P. Bhawal, S. Ganguly, T. Chaki, and N. Das, *RSC Adv.*, **6**, 20781 (2016).
(37) Y.-J. Wan, L.-C. Tang, D. Yan, L. Zhao, Y.-B. Li, L.-B. Wu, J.-X. Jiang, and G.-Q. Lai, *Compos. Sci. Technol.*, **82**, 60 (2013).
(38) Z. Chen and H. Lu, *J. Mater. Chem.*, **22**, 12479 (2012).
(39) S. Ganguly, P. Das, M. Bose, T. K. Das, S. Mondal, A. K. Das, and N. C. Das, *Ultrason. Sonochem.*, **39**, 577 (2017).
(40) S. Ganguly, S. Mondal, P. Das, P. Bhawal, T. kanti Das, M. Bose, S. Choudhary, S. Gangopadhyay, A. K. Das, and N. C. Das, *Nano-Structures & Nano-Objects*, **16**, 86 (2018).
(41) I. Roy, D. Rana, G. Sarkar, A. Bhattacharyya, N. R. Saha, S. Mondal, S. Pattanayak, S. Chattopadhyay, and D. Chattopadhyay, *RSC Adv.*, **5**, 25357 (2015).
(42) N. Wu, X. She, D. Yang, X. Wu, F. Su, and Y. Chen, *J. Mater. Chem.*, **22**, 17254 (2012).
(43) B. Shen, D. Lu, W. Zhai, and W. Zheng, *J. Mater. Chem. C*, **1**, 50 (2013).
(44) E.-Y. Choi, T. H. Han, J. Hong, J. E. Kim, S. H. Lee, H. W. Kim, and S. O. Kim, *J. Mater. Chem.*, **20**, 1907 (2010).
(45) L.-C. Tang, Y.-J. Wan, D. Yan, Y.-B. Pei, L. Zhao, Y.-B. Li, L.-B. Wu, J.-X. Jiang, and G.-Q. Lai, *Carbon*, **60**, 16 (2013).
(46) R. Giri, K. Naskar, and G. Nando, *Plastics, Rubber Compos.*, **41**, 341 (2012).
(47) S. Bhandari, N. K. Singha, and D. Khastgir, *J. Appl. Polym. Sci.*, **129**, 1264 (2013).
(48) A. Das and B. K. Satapathy, *Mater. Des.*, **32**, 1477 (2011).
(49) P. Dey, K. Naskar, B. Dash, S. Nair, G. Unnikrishnan, and G. B. Nando, *RSC Adv.*, **5**, 31886 (2015).
(50) T. Koga, T. Hashimoto, M. Takenaka, K. Aizawa, N. Amino, M. Nakamura, D. Yamaguchi and S. Koizumi, *Macromolecules*, **41**, 453 (2008).
(51) S. Ganguly and N. C. Das, *Polymer*, **61**, 192 (2015).
(52) S. Ganguly, P. P. Maity, S. Mondal, P. Das, P. Bhawal, S. Dhara and N. C. Das, *Mater. Sci. Eng. C*, **92**, 34 (2018).
(53) L. Karasek, B. Meissner, S. Asai, and M. Sumita, *Polym. J.*, **28**, 121 (1996).
(54) H. Kang, Y. Tang, L. Yao, F. Yang, Q. Fang, and D. Hui, *Compos. Part B: Eng.*, **112**, 1 (2017).
(55) X. Hu, E. Su, B. Zhu, J. Jia, P. Yao, and Y. Bai, *Compos. Sci. Technol.*, **97**, 6 (2014).
(56) F. W. Starr, T. B. Schrøder, and S. C. Glotzer, *Macromolecules*, **35**, 4481 (2002).
(57) G. D. Smith, D. Bedrov, L. Li, and O. Byutner, *J. Chem. Phys.*, **117**, 9478 (2002).
(58) T. Ramanathan, A. Abdala, S. Stankovich, D. Dikin, M. Herrera-Alonso, R. Piner, D. Adamson, H. Schniepp, X. Chen, and R. Ruoff, *Nat. Nanotechnol.*, **3**, 327 (2008).
(59) C.-C. Teng, C.-C. M. Ma, C.-H. Lu, S.-Y. Yang, S.-H. Lee, M.-C. Hsiao, M.-Y. Yen, K.-C. Chiou, and T.-M. Lee, *Carbon*, **49**, 5107 (2011).
(60) S. Donath, H. Militz, and C. Mai, *Holzforschung*, **60**, 40 (2006).

